Carbohydrate Polymers 94 (2013) 147–153

Contents lists available at SciVerse ScienceDirect

Carbohydrate Polymers

journal homepage: www.elsevier.com/locate/carbpol

Electrospun curcumin-loaded fibers with potential biomedical applications

Xiao-Zhu Sun [a], Gareth R. Williams [b], Xiao-Xiao Hou [a], Li-Min Zhu [a,*]

[a] College of Chemistry Chemical Engineering and Biotechnology, Donghua University, Shanghai 201620, PR China
[b] UCL School of Pharmacy, 29-39 Brunswick Square, London WC1N 1AX, UK

ARTICLE INFO

Article history:
Received 28 September 2012
Received in revised form
10 December 2012
Accepted 26 December 2012
Available online 3 January 2013

Keywords:
Electrospinning
Inclusion complex
Nanofiber
Polyvinyl alcohol (PVA)
Curcumin

ABSTRACT

Polyvinyl alcohol (PVA) nanofibers loaded with curcumin or its β-cyclodextrin (CD) inclusion complex were successfully prepared using an electrospinning process. The influence of curcumin or CD–curcumin complex content on fiber formation and quality was investigated. X-ray diffraction and differential scanning calorimetry analyses of the fibers, together with electron microscope evidence, demonstrated that curcumin is likely to be present as crystalline aggregates in the fibers, while its CD complex is more evenly distributed. ^{1}H NMR analysis indicated that the chemical structure of curcumin was preserved during the electrospinning process. Thermogravimetric analysis demonstrated that inclusion into nanofibers enhanced the thermal stability of curcumin. *In vitro* dissolution tests showed that the drug release profiles of the PVA/curcumin and PVA/complex fibers were different, with release from the latter occurring more rapidly. Release from both fiber types was found to be largely governed by a diffusion-controlled mechanism; two sequential stages for drug release were observed.

1. Introduction

Curcumin, derived from the rhizome of the plant curcuma longa, is a low molecular weight natural yellow-orange polyphenol compound. It is widely used in spices, cosmetics, and traditional Chinese medicine. A range of therapeutic properties have been identified for curcumin, including anti-inflammation, anti-oxidation and anti-cancer activities (Bar-Sela, Epelbaum, & Schaffer, 2010; Dhillon et al., 2008; Sharma, Steward, & Gescher, 2007; Tomren, Masson, Loftsson, & Tonnesen, 2007). Unfortunately, curcumin suffers from low solubility in water and is unstable to alkaline conditions, thermal treatment and light: these drawbacks usually limit its applications. In pharmaceutics, organic solvents generally need to be avoided, and hence routes to improve curcumin's solubility in aqueous solution are required to permit its therapeutic usage. A range of carriers have been explored to this end, based on incorporating curcumin in microgels, or employing surfactants, proteins, and lipids (Leung & Kee, 2009; Maiti, Mukherjee, Gantait, Saha, & Mukherjee, 2007; Shaikh, Ankola, Beniwal, Singh, & Kumar, 2009; Wang, Leung, Kee, & English, 2010).

Cyclodextrins (CDs), composed of six to eight linked D-glucopyranose units connected by 1,4-glycosidic bonds, possess hydrophobic cavities of different sizes, which render them capable of forming inclusion complexes with a range of hydrophobic compounds. This means that cyclodextrins can be used as drug carriers to increase the aqueous solubility and enhance the stability of guest molecules, such as curcumin (Paramera, Konteles, & Karathanos, 2011; Yallapu, Jaggi, & Chauhan, 2010). Complexes of curcumin and CDs have been shown to ameliorate the drawbacks mentioned above (Haiyee et al., 2009; Tomren et al., 2007). Curcumin is believed to form an inclusion complex with β-CD in a 2:1 host:guest molar ratio, where each of the two phenyl rings of the curcumin molecule is encapsulated in a separate CD host (Tang, Ma, Wang, & Zhang, 2002).

Electrospinning, a versatile and cost-effective method for producing nanoscale fibers, has received great attention in recent years. Electrospun nanofibers have many attractive properties such as a large surface-to-volume ratio, nanoporous structure, and flexibility for physical/chemical modification. This makes them applicable in various areas including tissue engineering, wound healing, drug delivery systems, membranes/filters, *inter alia* (Greiner & Wendorff, 2007; Jia et al., 2007; Reneker & Yarin, 2008; Yoon, Hsiao, & Chu, 2008). Nanofibrous membranes containing β-CD can be used for separation or filtration owing to their large surface areas and nanoporous structures (Uyar et al., 2009; Zhang, Chen, & Diao, 2011). In addition, higher thermal stability, prolonged shelf-lives and slow release properties have been observed for food additives incorporated into CD and subsequently embedded into electrospun nanofibers (Kayaci & Uyar, 2012). Electrospun curcumin fiber mats have been explored as anticoagulation membranes, antitumor agents, drug delivery systems and cell culture surfaces (Brahatheeswaran et al., 2012; Chen, Lin, Fei, Wang, & Gao,

* Corresponding author. Tel.: +86 21 67792655; fax: +86 21 67792655.
E-mail address: lzhu@dhu.edu.cn (L.-M. Zhu).

0144-8617/$ – see front matter © 2013 Elsevier Ltd. All rights reserved.
http://dx.doi.org/10.1016/j.carbpol.2012.12.064

2010; Guo et al., 2011; Suwantong, Opanasopit, Ruktanonchal, & Supaphol, 2007). As a result, it is clear that electrospun curcumin-containing fibers may offer enhancements in drug solubility and stability. To date, however, there are no reports of fibers containing the curcumin–CD complex, and it is not known how such fibers might compare to those containing curcumin alone. In this paper, we redress this deficiency in understanding. Curcumin or its CD inclusion complex were added into polyvinyl alcohol (PVA) solutions and subsequently fabricated into nanofibers by electrospinning. The drug-loaded fibers were assessed for their potential as carriers for the delivery of curcumin. The fiber morphology and the physical state of the drug in the fibers were probed both for the curcumin-loaded and the curcumin/CD-loaded fibers, and *in vitro* drug release profiles were investigated.

2. Experimental

2.1. Materials

PVA (1788) was purchased from the Aladdin Reagent Co. Ltd. (Shanghai, China). Curcumin and β-CD were purchased from the Sinopharm Chemical Reagent Co. Ltd. (Shanghai, China). Water was distilled before use. All other chemicals and reagents were of analytical grade.

2.2. Preparation of inclusion complexes

Curcumin was dissolved in a minimum volume of acetone at ambient temperature, and then added dropwise with continuous stirring to a flask containing a saturated aqueous solution of β-CD at 45 °C. The stoichiometry of curcumin and β-CD was fixed at 1:2. The mixture was refluxed with vigorous agitation at 50 °C for about 4 h. The solution was then stirred for an additional hour at 60 °C to remove acetone and cooled to room temperature. After stirring for a further 8 h at an ambient temperature, the mixture was stored overnight in the fridge and the solid product recovered *via* vacuum filtration. The crystalline product was dried in a vacuum oven at 37 °C for 12 h.

2.3. Preparation of spinning solutions

PVA/curcumin solutions were prepared by dissolving curcumin in a 10% (w/v) aqueous PVA solution. Solutions were prepared with curcumin at 5 wt%, 10 wt%, 15 wt% and 20 wt% with respect to the PVA content, and then stirred for 8 h at room temperature. PVA/CD complex solutions were prepared using analogous procedures, except that the amount of complex used was 20 wt%, 30 wt%, 40 wt% and 50 wt% with respect to the PVA content. All the solutions were degassed with a SK5200H ultrasonator (350W, Shanghai Jinghong Instrument Co. Ltd., Shanghai, China) for 5 min immediately before electrospinning.

2.4. Electrospinning process

The drug/polymer solutions were loaded into a 5 ml syringe. The syringe was fixed horizontally onto a syringe pump (Cole-Parmer®, IL, USA) and the solutions were electrospun using a high voltage power supply (Shanghai Sute Electrical Co. Ltd., Shanghai, China). Electrospinning was performed using the following parameters: applied voltage = 15 kV; tip-to-collector distance = 20 cm; solution flow rate = 0.5 ml/h; relative humidity = *ca.* 40%. The resultant fibers were dried at 37 °C in a vacuum oven (Shanghai Laboratory Instrument Work Co. Ltd., Shanghai, China) to facilitate the removal of residual water.

2.5. Characterization

The morphology and the diameter of the electrospun nanofibers were analyzed by scanning electron microscopy (SEM; JSM-5600LV, JEOL, Tokyo, Japan). Samples were gold sputter-coated under argon prior to imaging. The average fiber diameter for each sample was calculated by analysis of around 50 fibers in SEM images using the Image J software (National Institutes of Health, MD, USA).

Fourier transformed infrared spectroscopy (FTIR) was conducted using a Nicolet-Nexus 670 FTIR spectrometer (Nicolet Instrument Corporation, WI, USA) over the scanning range 500–4000 cm^{-1} with a resolution of 2 cm^{-1}.

X-ray diffraction (XRD) patterns were obtained on a D/Max-BR diffractometer (RigaKu, Tokyo, Japan) with Cu Kα radiation (40 mV/30 mA) over the 2θ range 5–60°.

Differential scanning calorimetry (DSC) analyses were carried out using an MDSC 2910 differential scanning calorimeter (TA Instruments Co., DE, USA). Sealed samples were heated under nitrogen at 10 °C/min from 20 to 250 °C. The nitrogen flow rate was 40 ml/min.

Thermogravimetric data were recorded on a TG209F1 thermogravimetric analyzer (TA Instruments Co., DE, USA) from 20 to 700 °C at a heating rate of 20 °C/min, under a nitrogen atmosphere.

^{1}H NMR spectra were obtained in DMSO-d6 using a Bruker DRX 400 MHz NMR spectrophotometer.

2.6. In vitro drug release

Experiments were conducted at 37 °C and 100 rpm in a thermostatic shaking incubator (Jintan Instrument Co. Ltd., Jiangsu, China) in 200 ml of the release medium (pH 6.8 phosphate buffer with 0.5% (v/v) Tween 80). Control experiments were performed in which 1.45 mg of curcumin was added to the medium, and then experiments conducted with the following amounts of PVA/curcumin fibers: 30.5 mg (5 wt%), 16.0 mg (10 wt%), 11.1 mg (15 wt%) and 8.6 mg (20 wt%). Similarly, experiments were performed with PVA/complex fibers using 71.6 mg (20 wt%), 51.7 mg (30 wt%), 41.8 mg (40 wt%) and 35.8 mg (50 wt%) of material. At predetermined time intervals, aliquots of 5 ml were withdrawn for sampling and replaced by an equal volume of the release medium to maintain a constant volume. After filtration through a membrane (0.45 μm), the sample solutions were analyzed at a wavelength of 426 nm by a UV spectrophotometer (Unico Instrument Co. Ltd., Shanghai, China). The amount of drug present in the sample was calculated using calibration curves. The amount of drug released was plotted as the percentage released *versus* time. All measurements were conducted in triplicate, and results are reported as average values ± S.D.

3. Results and discussion

3.1. Morphology and fiber size

After some initial optimization, a range of PVA nanofibers containing curcumin or β-CD–curcumin complexes were successfully electrospun from aqueous solutions. Representative SEM images of PVA/curcumin and PVA/CD–curcumin fibers are depicted in Fig. 1(a)–(h). The fiber diameter distributions are presented in Fig. 1(i).

In the case of PVA/curcumin fibers, while the 5 wt% fibers have smooth structures with no visible beading, some “bead on string” features are observed with higher drug loading. The number of beads on the nanofibers is generally observed to increase with the amount of curcumin, possibly due to the low solubility of curcumin causing aggregation in the spinning solutions. The average fiber

diameters are between 250 and 350 nm, with fiber size reducing as the curcumin content is increased. This may be a result of solution conductivity rising with the addition of curcumin (Suwantong et al., 2007).

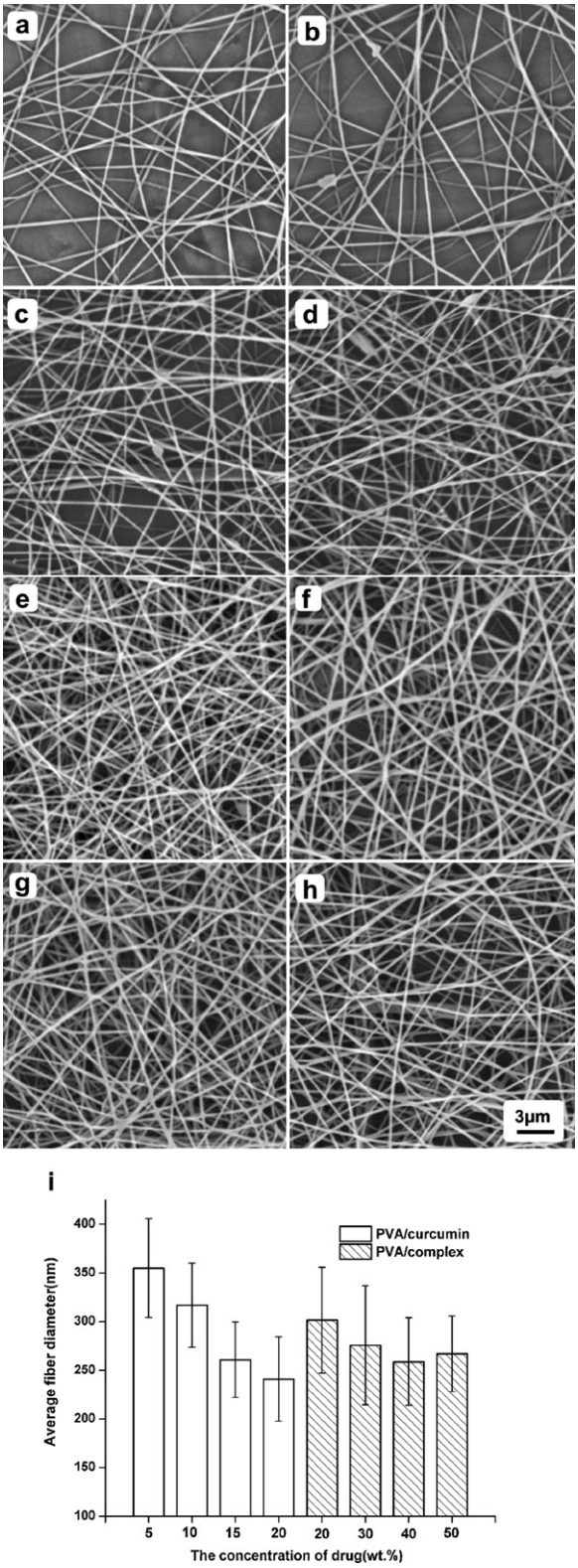

Fig. 1. SEM images of curcumin-loaded PVA nanofibers with: (a) 5 wt.%, (b) 10 wt.%, (c) 15 wt.%, (d) 20 wt.% drug content, and complex-loaded fibers containing: (e) 20 wt.%, (f) 30 wt.%, (g) 40 wt.%, (h) 50 wt.% complex. (i) Average fiber diameter of the various fibers. Error bars depict one standard deviation.

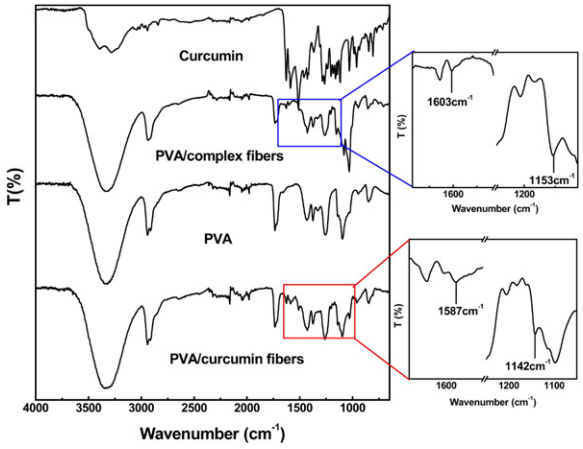

Fig. 2. FTIR spectra of curcumin, PVA, together with the 10 wt% PVA/curcumin and 50 wt% PVA/complex nanofibers.

For the PVA/complex system, uniform and smooth nanofibers were obtained in all cases (see Fig. 1(e)–(h)). It is presumed that the CD–curcumin complex is evenly distributed in the spinning solutions owing to the increased solubility of the inclusion complex and interactions between PVA and cyclodextrin. The average fiber diameters (Fig. 1(i)) tend to decrease with increasing CD–curcumin content, following the same general trend as observed for the PVA/curcumin system. However, only a small reduction in diameters is seen for PVA/complex fibers, from 300 nm at 20 wt% to around 260 nm at 50 wt%. This may be a consequence of hydrogen bonding between PVA and β-CD causing the spinning solution to increase in viscosity, counteracting the conductivity enhancement effect of curcumin (Zhang et al., 2011).

3.2. Further characterization

FTIR spectra for PVA, curcumin and the nanofibers of PVA/curcumin and PVA/complex are shown in Fig. 2. The spectrum of PVA has characteristic peaks from —OH at 3319 cm^{-1}, stretching vibrations of CH_2/CH groups at 2941/2912 cm^{-1} and of C=O at 1734 cm^{-1}, together with deformation bands of CH_2/CH at 1435/1375 cm^{-1}, and C—O stretching vibrations at 1096 cm^{-1} and 1258 cm^{-1}.

For curcumin, the bands observed at 3085–3552 cm^{-1}, 1588 cm^{-1}, 1512 cm^{-1}, 1265 cm^{-1}, and 1143 cm^{-1} are respectively attributed to the phenolic O—H stretching, stretching vibrations of the benzene ring, C=C vibrations, aromatic C—O stretching and C—O—C stretching modes.

The spectrum of the 10 wt% PVA/curcumin fiber is given in Fig. 2. The spectra of all the PVA/curcumin fibers show the same features. They comprise a composite of the PVA and curcumin spectra, displaying all the characteristic bands of both PVA and curcumin. This indicates few interactions occur between the two components.

In contrast, there are some additional features visible in the spectra of the PVA/complex fibers; the spectrum for the 50 wt% fiber is provided in Fig. 2, and the spectra of the other fibers show the same features. The appearance of sharp peaks at 1032 cm^{-1} corresponds to the C—O—C glucose units of β-CD. The characteristic peaks of the benzene ring and C—O—C groups which are found at 1587 cm^{-1} and 1142 cm^{-1} for pure curcumin have shifted to 1603 cm^{-1} and 1153 cm^{-1} in the CD–curcumin fibers. These changes can be attributed to the encapsulation of the phenyl ring at the ends of the curcumin molecule by the β-CD.

X-ray diffraction patterns of curcumin and PVA, together with the PVA/curcumin and PVA/complex nanofibers are presented in Fig. 3. Pure curcumin exists in a crystalline state, displaying a

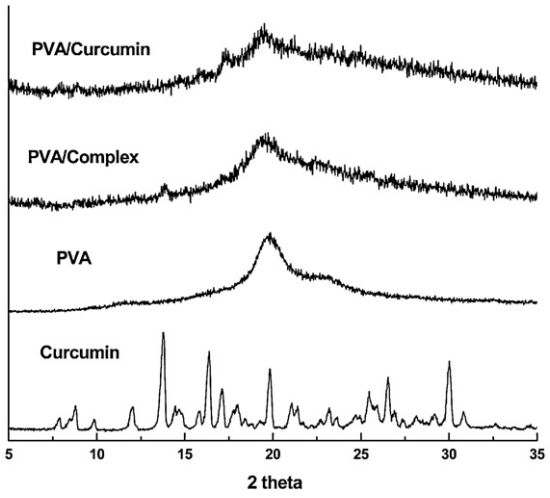

Fig. 3. X-ray diffraction patterns of curcumin and PVA, together with the 10 wt% PVA/curcumin and 50 wt% PVA/complex fibers.

number of characteristic reflections between 10° and 30° 2θ. PVA displays only a broad diffraction halo between 17° and 25°, typical of its semi-crystalline nature. Both the PVA/curcumin and PVA/complex XRD patterns show some small diffraction peaks, which may be attributed to raw curcumin, suggesting that some of the curcumin is still present in a crystalline state in the fibers. The PVA/complex nanofibers do not show any of the characteristic peaks for curcumin, but some new reflections (*e.g.* at 13.84°) are visible, suggesting that both curcumin and the CD–curcumin complex have at least some crystalline nature in the fibers.

The ^{1}H NMR spectra of curcumin, PVA, PVA/curcumin and PVA/complex nanofibers are shown in Fig. 4. Curcumin exhibits proton signals at δ 3.84 (Hf, —OMe), δ 6.06 (Hg), δ 6.74–7.56 (Hh), δ 9.66 (Hi, —OH) and δ 16.4 (Hj, —OH) (Peret-Almeida, Cherubino, Alves, Dufosse, & Gloria, 2005). PVA shows proton signals at δ 1.28–1.69 (Ha), δ 1.94–2.00 (Hb), δ 3.83–3.89 (Hc, Hd), and δ 4.23–4.67 (He, —OH) (Gholap, Jog, & Badiger, 2004). Following dissolution of the PVA/curcumin fibers, all the resonances of PVA and curcumin appear at the same chemical shift values, suggesting that the chemical integrity of curcumin was retained after elecrospinning.

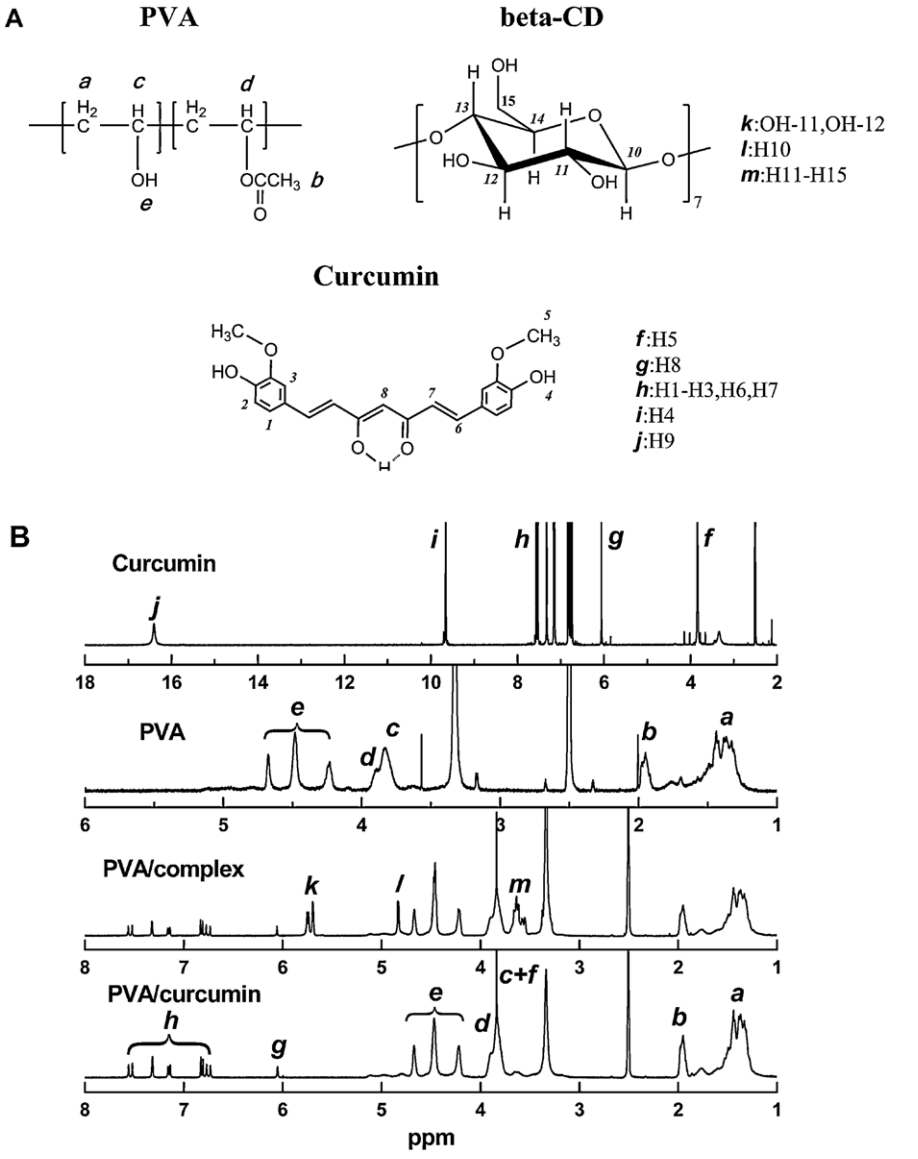

Fig. 4. (A) chemical structures and (B) ^{1}H NMR spectra of curcumin, PVA, 10 wt% PVA/curcumin and 50 wt% PVA/complex fibers.

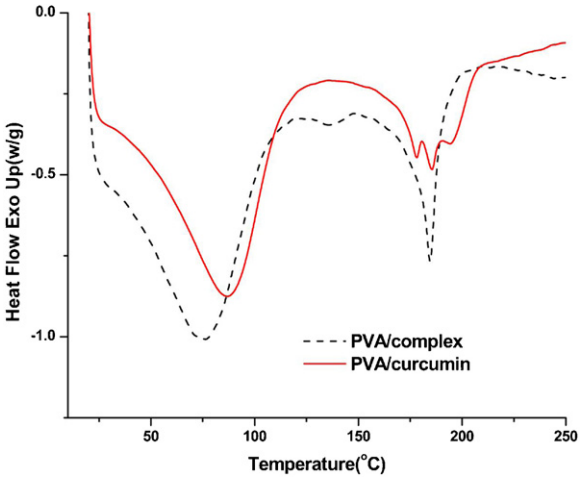

Fig. 5. DSC thermograms of the 10 wt% PVA/curcumin and 50 wt% PVA/complex nanofibers. (For interpretation of the references to color in the text, the reader is referred to the web version of the article.)

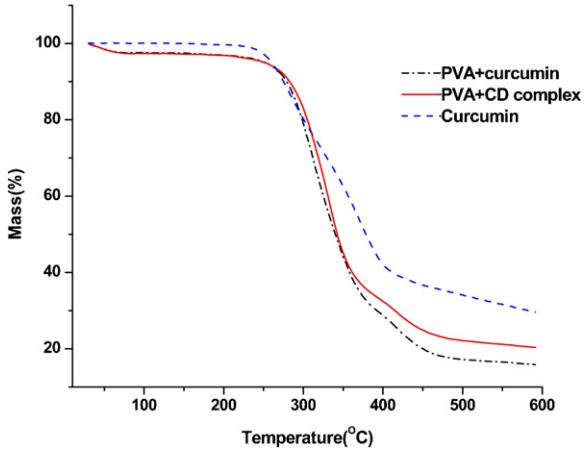

Fig. 6. TGA traces of curcumin, 10 wt% PVA/curcumin and 50 wt% PVA/complex fibers. (For interpretation of the references to color in the text, the reader is referred to the web version of the article.)

The PVA/complex nanofibers present several extra chemical shifts following their dissolution in DMSO. Additional peaks are visible at 3.58–3.66, 4.83, and 5.73–5.75 ppm, and correspond to the proton signals of Hm, Hl, Hk from the β-CD. The hydroxyl resonance of β-CD (Hk) exhibits a small splitting as a result of hydrogen bonding interactions between PVA and β-CD (Horvath et al., 2008). Due to its high solubility in DMSO, curcumin is removed from the complex in the course of NMR sample preparation, which results in the signals for curcumin being clearly visible in the NMR of the dissolved PVA/complex fibers.

The DSC thermograms of the 10 wt% PVA/curcumin (red solid line) and 50 wt% PVA/complex (black dash line) fibers are depicted in Fig. 5. The PVA/curcumin thermogram has a broad endothermic peak between 50 and 100 °C due to loss of water, two endothermic peaks at around 178 and 185 °C corresponding to the melting temperatures (Tm) of curcumin and PVA respectively and a thermal decomposition peak of curcumin at 194 °C. A phase separation between the two components in the fiber is clearly observed here, in agreement with the results of X-ray diffraction.

In contrast, in the thermogram of the PVA/complex fibers, the Tm peak of curcumin at 178 °C is not visible, which indicates the generation of a homogenous system with the action of CD; the water evaporation endotherm has also been shifted to lower temperature, from 87 to *ca.* 76 °C. This can be attributed to CD molecules taking over some binding sites of water molecules in PVA on account of its stronger interaction with PVA.

The thermogravimetric analysis curves of curcumin (blue dash line), 10 wt% PVA/curcumin (black dash shot line) and 50 wt% PVA/complex fibers (red solid line) are shown in Fig. 6.

The TGA trace of the PVA/curcumin fibers is very similar to that of the complex-containing fibers; both show water loss below 100 °C and a decomposition process starting at around 270 °C and continuing to 500 °C, as a result of thermal degradation of PVA and curcumin. The onset of degradation is at a higher temperature than with raw curcumin, where degradation starts at 245 °C, indicating enhanced thermal stability.

3.3. *In vitro* release

Release profiles of curcumin and the CD–curcumin complex from the electrospun fiber mats are included in Fig. 7Aand B.

Considering first the PVA/curcumin fibers, it is found that the fibers containing 5 wt% curcumin release the embedded drug most rapidly; the release percentage is close to 100% after 160 min. In contrast, the percentage release reaches only 83% for the 10 wt% fiber in this time period. Release from the 15 and 20 wt% fibers is slightly slower than from the 10 wt% fibers. The release rates of the curcumin lie in the order: 5 wt% > 10 wt% > 15 wt% ≈ 20 wt%. The higher solubility of the fibers compared to pure curcumin serves to accelerate drug release, as demonstrated by the fact that all the fibers release more rapidly than the pure drug dissolves.

The results may be rationalized in terms of the local structure of the fibers. Both XRD and DSC indicate that the curcumin was at least partially present in a crystalline state in the fibers. The larger the drug content in the fibers is, the greater the amount of crystalline material present. Since crystalline curcumin has poor solubility in the dissolution medium, it will be difficult for this to dissolve from the fibers. In contrast, for the 5 wt% fibers, curcumin is mainly present as small aggregates or in an amorphous state such that lower lattice energies need to be overcome for dissolution, and resulting in a relatively larger release rate.

Generally, the drug release curves of the PVA/complexes nanofibers are similar: an initial burst release is followed by a more gradual release period. Faster release, and a greater extent of release, is seen with higher complex loadings. This is thought to be caused by an increased curcumin content leading to a larger concentration gradient, and hence a higher diffusion driving force encouraging drug release. Compared to the PVA/curcumin fibers, curcumin release is more rapid with the PVA/complex fibers, (*cf.* Fig. 7A and 7B). This should lead to a higher systemic bioavailability and enhanced *in vivo* efficacy.

To assess the mechanism of drug release, the release percentage of curcumin or its CD complex was plotted against the square root of time in accordance with the Higuchi model (Wang, Wang, Chen, & Yun, 2008). According to this model, if drug release occurs *via* a diffusion-controlled mechanism a linear graph should be obtained (Suwantong et al., 2007; Xu, Chen, Ma, Wang, & Jing, 2008). As demonstrated in Fig. 7C, the release profiles consist of two sequential stages. There are clear linear relationships ($R^2 \geq 0.956$) between release rate and $t^{1/2}$ for both the first and second stages, with the first stage presenting a steeper slope than the second. This can be explained as follows: drug molecules located adjacent to the surface of the fibers or bound loosely on the surface have a larger diffusion rate and are released in the initial period. In the second stage of release, a longer time is required for drug molecules deep in the interior of fibers to reach the surface (requiring the degradation of some polymer units), and hence the release rate is slower.

The R^2 values for release from PVA/curcumin or PVA/complex fibers are listed in Table 1. The first stage of release tends to have

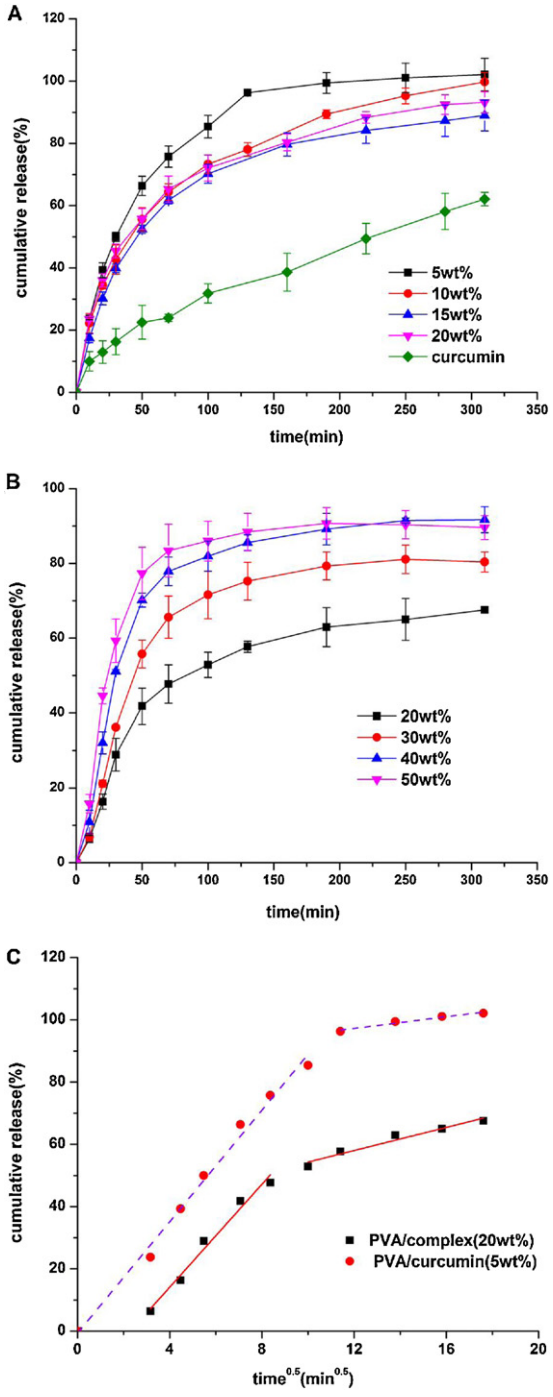

Fig. 7. *In vitro* dissolution profiles of (A) PVA/curcumin and (B) PVA/complex nanofibers; (C) selected release profiles plotted against the square root of time.

Table 1
R^2 values for the fitting of the Higuchi equation to the release data.

Fiber components	Drug content	Release stage	
		1	2
PVA/curcumin	5 wt%	0.994	0.967
	10 wt%	0.996	0.975
	15 wt%	0.991	0.997
	20 wt%	0.990	0.960
PVA/complex	20 wt%	0.981	0.956
	30 wt%	0.991	0.961
	40 wt%	0.991	0.971
	50 wt%	0.971	0.981

a greater R^2 value than the second, suggesting that it matches more closely to the Higuchi model, controlled by a Fickian diffusion mechanism. Polymer dissolution usually involves the processes of absorption of water, swelling, and disentanglement. The channels to release drugs will be mostly generated in the former two processes (adsorption/swelling), corresponding to the first stage of the release profile, while the bulk of channels will be broken with the erosion of polymer in the second stage. Thus, drug release is likely to be controlled by a combination of diffusion and erosion mechanisms.

4. Conclusions

In this study, nanofibers containing polyvinyl alcohol (PVA) and curcumin or PVA with a cyclodextrin–curcumin complex were successfully prepared by electrospinning. Scanning electron microscopy, X-ray diffraction and differential scanning calorimetry analysis suggested that curcumin was present as crystalline aggregates, while the CD complex was more highly distributed in its nanofibers. The PVA/curcumin fiber diameter was found to decrease rapidly with increasing curcumin content, while the PVA/complex fibers exhibited a small reduction in fiber diameter with increasing complex content. ^{1}H NMR spectra suggested that the chemical integrity of the curcumin was retained after electrospinning in both sets of fibers. Thermogravimetric analysis demonstrated that inclusion into nanofibers improved the thermal stability of curcumin. Sustained release of curcumin or its complex from the fibers occurs over 5 h, with two sequential stages of drug release observed. Drug release seems to be mainly governed by a diffusion-controlled mechanism. Our results show that the PVA/curcumin and PVA/complex nanofibers offer enhanced drug stability and solubility, and therefore have the potential to be developed in drug delivery, wound healing, and as promising materials for treating cancers.

Acknowledgements

This work was financially supported by the UK–China Joint Laboratory for Therapeutic Textiles (based at Donghua University), and the Biomedical Textile Materials “111 project” of the Ministry of Education of P.R. China (B07024).

References

Bar-Sela, G., Epelbaum, R., & Schaffer, M. (2010). Curcumin as an anti-cancer agent: Review of the gap between basic and clinical applications. *Current Medicinal Chemistry*, *17*(3), 190–197.

Brahatheeswaran, D., Mathew, A., Aswathy, R. G., Nagaoka, Y., Venugopal, K., Yoshida, Y., et al. (2012). Hybrid fluorescent curcumin loaded zein electrospun nanofibrous scaffold for biomedical applications. *Biomedical Materials*, *7*(4).

Chen, Y., Lin, J., Fei, Y. N., Wang, H. B., & Gao, W. D. (2010). Preparation and characterization of electrospinning PLA/Curcumin composite membranes. *Fibers and Polymers*, *11*(8), 1128–1131.

Dhillon, N., Aggarwal, B. B., Newman, R. A., Wolf, R. A., Kunnumakkara, A. B., Abbruzzese, J. L., et al. (2008). Phase II trial of curcumin in patients with advanced pancreatic cancer. *Clinical Cancer Research*, *14*(14), 4491–4499.

Gholap, S. G., Jog, J. P., & Badiger, M. V. (2004). Synthesis and characterization of hydrophobically modified poly(vinyl alcohol) hydrogel membrane. *Polymer*, *45*(17), 5863–5873.

Greiner, A., & Wendorff, J. H. (2007). Electrospinning: A fascinating method for the preparation of ultrathin fibres. *Angewandte Chemie: International Edition*, *46*(30), 5670–5703.

Guo, G., Fu, S. Z., Zhou, L. X., Liang, H., Fan, M., Luo, F., et al. (2011). Preparation of curcumin loaded poly(epsilon-caprolactone)–poly(ethylene glycol)–poly(epsilon-caprolactone) nanofibers and their in vitro antitumor activity against Glioma 9L cells. *Nanoscale*, *3*(9), 3825–3832.

Haiyee, Z. A., Saim, N., Said, M., Illias, R. M., Mustapha, W. A. W., & Hassan, O. (2009). Characterization of cyclodextrin complexes with turmeric oleoresin. *Food Chemistry*, *114*(2), 459–465.

Horvath, G., Premkumar, T., Boztas, A., Lee, E., Jon, S., & Geckeler, K. E. (2008). Supramolecular nanoencapsulation as a tool: Solubilization of the

anticancer drug trans-dichloro(dipyridine)platinum(II) by complexation with beta-cyclodextrin. *Molecular Pharmaceutics*, *5*(2), 358–363.

Jia, Y. T., Gong, J., Gu, X. H., Kim, H. Y., Dong, J., & Shen, X. Y. (2007). Fabrication and characterization of poly(vinyl alcohol)/chitosan blend nanofibers produced by electrospinning method. *Carbohydrate Polymers*, *67*(3), 403–409.

Kayaci, F., & Uyar, T. (2012). Encapsulation of vanillin/cyclodextrin inclusion complex in electrospun polyvinyl alcohol (PVA) nanowebs: Prolonged shelf-life and high temperature stability of vanillin. *Food Chemistry*, *133*(3), 641–649.

Leung, M. H. M., & Kee, T. W. (2009). Effective stabilization of curcumin by association to plasma proteins: Human serum albumin and fibrinogen. *Langmuir*, *25*(10), 5773–5777.

Maiti, K., Mukherjee, K., Gantait, A., Saha, B. P., & Mukherjee, P. K. (2007). Curcumin–phospholipid complex: Preparation, therapeutic evaluation and pharmacokinetic study in rats. *International Journal of Pharmaceutics*, *330*(1-2), 155–163.

Paramera, E. I., Konteles, S. J., & Karathanos, V. T. (2011). Stability and release properties of curcumin encapsulated in Saccharomyces cerevisiae, beta-cyclodextrin and modified starch. *Food Chemistry*, *125*(3), 913–922.

Peret-Almeida, L., Cherubino, A. P. F., Alves, R. J., Dufosse, L., & Gloria, M. B. A. (2005). Separation and determination of the physico-chemical characteristics of curcumin, demethoxycurcumin and bisdemethoxycurcumin. *Food Research International*, *38*(8-9), 1039–1044.

Reneker, D. H., & Yarin, A. L. (2008). Electrospinning jets and polymer nanofibers. *Polymer*, *49*(10), 2387–2425.

Shaikh, J., Ankola, D. D., Beniwal, V., Singh, D., & Kumar, M. N. V. R. (2009). Nanoparticle encapsulation improves oral bioavailability of curcumin by at least 9-fold when compared to curcumin administered with piperine as absorption enhancer. *European Journal of Pharmaceutical Sciences*, *37*(3–4), 223–230.

Sharma, R. A., Steward, W. P., & Gescher, A. J. (2007). Pharmacokinetics and pharmacodynamics of curcumin. *Molecular Targets and Therapeutic Uses of Curcumin in Health and Disease*, *595*, 453–470.

Suwantong, O., Opanasopit, P., Ruktanonchal, U., & Supaphol, P. (2007). Electrospun cellulose acetate fiber mats containing curcumin and release characteristic of the herbal substance. *Polymer*, *48*(26), 7546–7557.

Tang, B., Ma, L., Wang, H. Y., & Zhang, G. Y. (2002). Study on the supramolecular interaction of curcumin and beta-cyclodextrin by spectrophotometry and its analytical application. *Journal of Agricultural and Food Chemistry*, *50*(6), 1355–1361.

Tomren, M. A., Masson, M., Loftsson, T., & Tonnesen, H. H. (2007). Studies on curcumin and curcuminoids XXXI. Symmetric and asymmetric curcuminoids: Stability, activity and complexation with cyclodextrin. *International Journal of Pharmaceutics*, *338*(1–2), 27–34.

Uyar, T., Havelund, R., Nur, Y., Hacaloglu, J., Besenbacher, F., & Kingshott, P. (2009). Molecular filters based on cyclodextrin functionalized electrospun fibers. *Journal of Membrane Science*, *332*(1-2), 129–137.

Wang, J. X., Wang, Z. H., Chen, J. F., & Yun, J. (2008). Direct encapsulation of water-soluble drug into silica microcapsules for sustained release applications. *Materials Research Bulletin*, *43*(12), 3374–3381.

Wang, Z. F., Leung, M. H. M., Kee, T. W., & English, D. S. (2010). The role of charge in the surfactant-assisted stabilization of the natural product curcumin. *Langmuir*, *26*(8), 5520–5526.

Xu, X. L., Chen, X. S., Ma, P. A., Wang, X. R., & Jing, X. B. (2008). The release behavior of doxorubicin hydrochloride from medicated fibers prepared by emulsion-electrospinning. *European Journal of Pharmaceutics and Biopharmaceutics*, *70*(1), 165–170.

Yallapu, M. M., Jaggi, M., & Chauhan, S. C. (2010). beta-Cyclodextrin-curcumin self-assembly enhances curcumin delivery in prostate cancer cells. *Colloids and Surfaces B: Biointerfaces*, *79*(1), 113–125.

Yoon, K., Hsiao, B. S., & Chu, B. (2008). Functional nanofibers for environmental applications. *Journal of Materials Chemistry*, *18*(44), 5326–5334.

Zhang, W., Chen, M., & Diao, G. W. (2011). Electrospinning beta-cyclodextrin/poly(vinyl alcohol) nanofibrous membrane for molecular capture. *Carbohydrate Polymers*, *86*(3), 1410–1416.